



Get Clarity On Generics

Cost-Effective CT & MRI Contrast Agents



FRESENIUS
KABI

WATCH VIDEO

AJNR

Radiologic-pathologic correlation. Diffuse pontine astrocytoma.

A G Kane, H A Robles, J G Smirniotopoulos, J D Heironimus and M H Fish

AJNR Am J Neuroradiol 1993, 14 (4) 941-945

<http://www.ajnr.org/content/14/4/941>

This information is current as
of August 9, 2025.

Radiologic-Pathologic Correlation

Diffuse Pontine Astrocytoma

Arthur G. Kane,¹ Hector A. Robles, James G. Smirniotopoulos, James D. Heironimus, and Melton H. Fish

From the Departments of Radiology (AGK), Nuclear Medicine (JDH), and Pathology (MHF), Brooke Army Medical Center, San Antonio, TX; Department of Radiology, Walter Reed Army Medical Center, Washington, DC (HAR); and Department of Radiologic Pathology, Armed Forces Institute of Pathology, Washington, DC (JGS)

Clinical History

A 5-year-old girl presented with a several-month history of slurred speech, attention deficit, gait abnormalities, and visual problems. Computed tomography (CT) scan without contrast was obtained (Fig 1). A magnetic resonance (MR) scan was then obtained; it revealed diffuse enlargement of the pons, which was slightly hypointense on T1 (600/27) (TR/TE)-weighted images and hyperintense on T2-(2500/80) and proton density (2500/30)-weighted images. There was no appreciable enhancement after gadolinium administration. Without a biopsy, the patient underwent cisplatin chemotherapy and radiation therapy twice a day for 6 weeks, for the presumed diagnosis of brain stem glioma. The patient experienced remission of symptoms and was started on steroid treatment. Serial MR scans at 1, 2, and 4 months after initial therapy revealed a slight reduction in the mass effect of the tumor without any change in signal and without enhancement or development of any other abnormality.

However, an MR scan performed 7 months after therapy revealed marked enhancement in

the central pons. To differentiate between regrowth of tumor and radiation necrosis or non-neoplastic causes of enhancement, thallium-201 (²⁰¹Tl) single-photon emission CT (SPECT) was performed (Fig 2). This was interpreted as showing increased uptake in the pons consistent with regrowth of tumor.

The patient improved, but symptoms recurred 9 months after therapy, to include right-sided extremity weakness, dysphagia, nausea, and vomiting. MR scan at that time revealed enhancement in the pons increased over that noted at 8 months as well as enlargement of the lateral ventricles consistent with hydrocephalus. A ventriculoperitoneal shunt was placed, after which the patient became more alert and regained some function in the right upper and lower extremity. Bone marrow harvest was performed to allow intense multi-

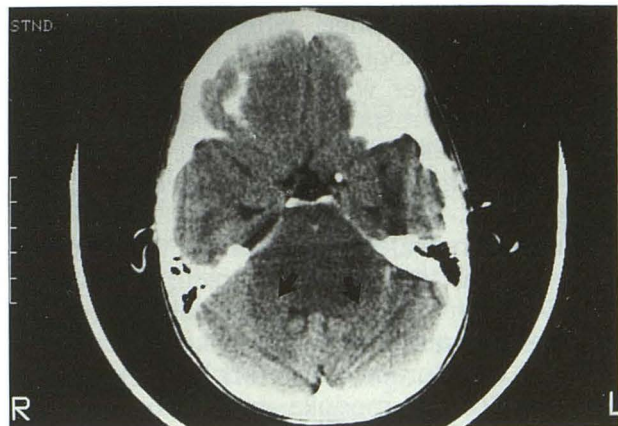


Fig. 1. Noncontrast axial CT scan through the level of the pons before therapy reveals a poorly defined low-density mass within the pons with mild expansion of the brain stem (arrow).

The opinions or assertions contained herein are the private views of the authors and are not to be construed as reflecting the views of the Department of the Army or the Department of Defense.

¹ Address reprint requests to Arthur G. Kane, MD, Captain, Department of Radiology, Brooke Army Medical Center, San Antonio, TX 78234.

Index terms: Brain stem, neoplasms; Radiologic-pathologic correlations

AJNR 14:941-945, Jul/Aug 1993 0195-6108/93/1404-0941

© American Society of Neuroradiology

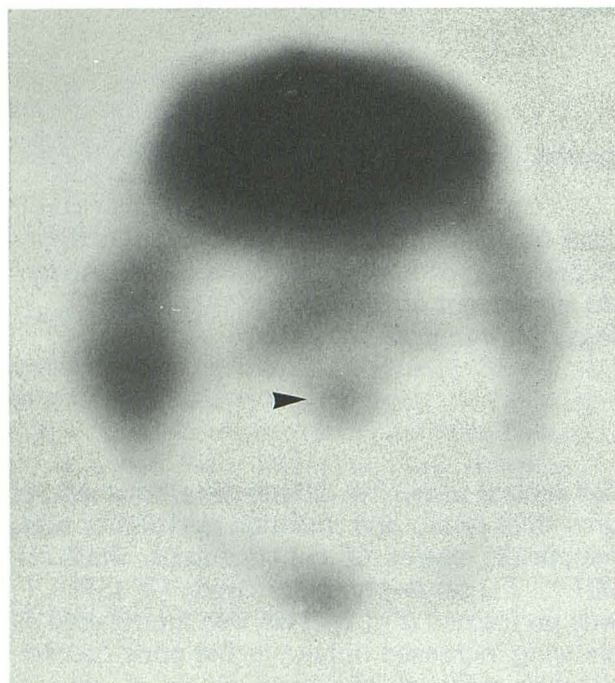


Fig. 2. Axial ^{201}Tl -SPECT image through the brain stem 8 months after initial therapy reveals increased uptake in the region of the pons (arrowhead), consistent with regrowth of tumor.

regimen chemotherapy. One week later, the patient underwent infusion with her autologous bone marrow, after which she showed worsening symptoms, which improved with steroid therapy. MR performed at that time (10 months after initial therapy) confirmed reduction of the hydrocephalus but persistent enhancement on postcontrast study. Over the next 3 weeks the patient developed progressive respiratory difficulty with tachypnea, wheezing, and worsening of neurologic symptoms. A "do-not-resuscitate" order was written in light of the patient's poor response to maximal therapy and of the results of an MR scan performed at that time (Figs 3-5). The following day, the patient died.

Autopsy revealed symmetrical nodular enlargement of the pons and the medulla (Fig 4B). Sectioning of the pons revealed a central pontine hematoma (Fig 5B) surrounded by necrosis and tumor. The neoplasm extended into the midbrain, medulla, and cerebellar white matter via the middle cerebellar peduncles (Fig 5B). Histologic exam revealed diffuse pontine fibrillary astrocytoma (grade II/IV) with extensive necrosis and surrounding areas of hemorrhage (Fig 6).

General Discussion

Brain stem tumors comprise approximately 10% to 15% of infratentorial central nervous system neoplasms in the pediatric population (1, 2). The natural history of brain stem glioma is a progression of the disease with a median survival of only 4 to 15 months (3, 4). Most (75%) occur before the age of 10, with a median age of presentation being approximately 6 years, and a predominant number of cases occurring in males (2.5:1) (2). Even with radiation and chemotherapy, the overall 5-year survival in histologically documented lesions is 5% (5). Although the prognosis remains poor, early diagnosis may result in improved survival with treatment. Classic presenting symptoms may include headaches, nausea, vomiting, gait disturbance, ataxia, visual deficits, seizures, hemiparesis, and cranial nerve dysfunction (6). Occasionally more bizarre isolated symptoms may lead one to suspect a brain stem lesion (7). The average duration of symptoms at diagnosis is 3 to 4 months (6).

Location

Brain stem gliomas most commonly originate in or involve the pons (54%), followed in frequency by the medulla (32%); infrequently they involve the mesencephalon (5). Pontine gliomas and mesencephalic gliomas often extend superiorly into the thalamus, inferiorly into the medulla, or posterolaterally through the cerebellar peduncles into the cerebellar hemisphere (Fig 5B) (8, 9).

Pathology

Gross

Although often diffusely infiltrating, pontine glioma also can demonstrate marked exophytic growth (Fig 4) into the cerebellopontine angle, cisterna magna, perimesencephalic cistern, or vallecule in up to 60% of cases (10). The basilar artery is frequently engulfed by the tumor and eventually lies within a deep ventral groove (Figs 3, 4A, and 5) (8, 10). Single or multiple cysts can be found in up to one-fourth of brain stem gliomas (10, 11). Recent and old hemorrhage is common, but calcification is rare (Figs 3-5) (9, 11). The expansion of the pons by the tumor tends to flatten the fourth

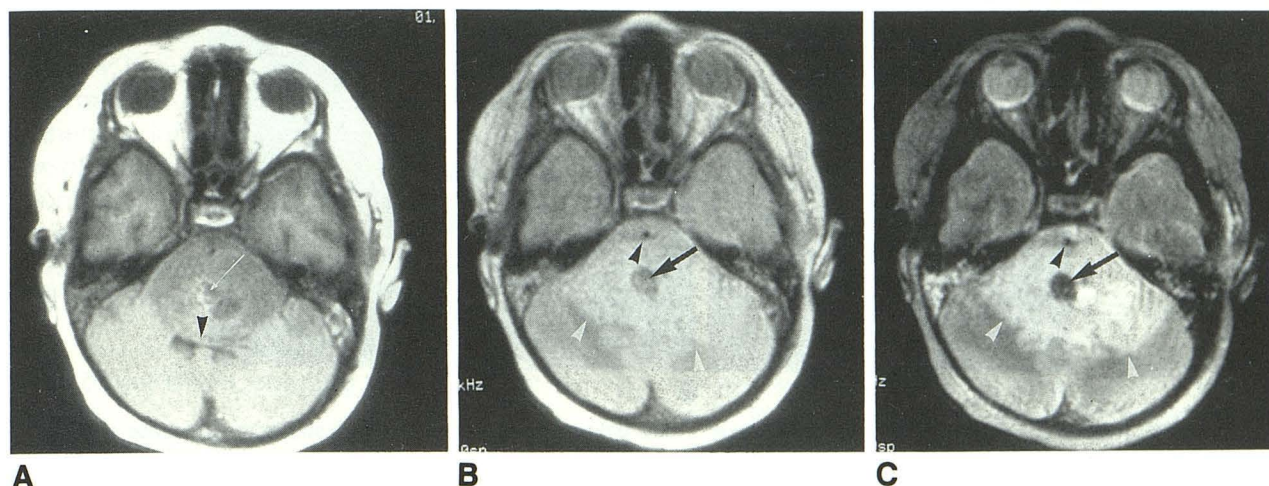


Fig. 3. A, MR axial T1-weighted image (spin echo (SE) 600/27) 1 day before the patient's death demonstrates low signal in the pons with central focal hyperintense signal (*small white arrow*) in the central pons. There is mass effect of the pontine glioma on the fourth ventricle (*black arrowhead*). The central focus demonstrates signal loss on (B) (*arrow*) a proton density (SE 2500/30)-weighted image and becomes even darker with increasingly T2-weighted (SE 2500/80) image (C) (*arrow*). This is consistent with early subacute hematoma (predominantly deoxyhemoglobin with some intracellular methemoglobin). Note that the surrounding area of hyperintensity (*white arrowhead*) in the double-echo images is much larger than the portions of hypointense pons on axial T1-weighted image. The basilar artery (*black arrowheads*) in B and C is engulfed by tumor.

ventricle and the pontine tegmentum may become convex posteriorly. However, hydrocephalus is rare unless the tumor involves the midbrain (Fig 3).

Microscopic

Brain stem gliomas are typically low-grade malignancies but can be high grade. Tumor cells tend to infiltrate diffusely in intimate association with the existing neurons and blood vessels (Figs 6A and 6B). Histologic grade is based on the degree of anaplasia or dedifferentiation, number of mitoses, and presence of necrosis (12–14).

The delayed effects of radiation and chemotherapy are varied, but demyelination with a reduction of glial parenchymal elements and damage to peripheral vessels leading to necrosis and infarction in zones of radiation are characteristic (Fig 6C) (15). Brain stem tumors that have focal involvement or are exophytic may have a more favorable prognosis in that they tend to be low grade and are often amenable to surgical resection (12–14).

Imaging

CT

Brain stem tumors almost always appear as a focally expanded hypodense area in the brain

stem on CT (Fig 1). The presence of contrast enhancement before treatment is variable and apparently does not predict alteration of survival time (13). However, two CT features, hypodensity and involvement of the entire brain stem, have correlated with a worse prognosis (13). CT may be more sensitive than MR in the detection of acute hemorrhage within the brain stem, whereas MR may be more sensitive in the early subacute to late stage of hemorrhage (Figs 3–5) (16).

MR

Many of the lesions in the differential diagnosis for an intra-axial brain stem lesion have the effect of lengthening both the T1 and T2 relaxation times of adjacent brain stem tissue. In brain stem tumors, however, the area of abnormal signal on T2-weighted images is usually more extensive than the areas of abnormal signal on T1-weighted images. Except in cases of hemorrhage, the advantage of MR in characterizing a brain stem lesion lies in its ability to demonstrate lesion location, focality, and morphology—features often obscured by CT because of beam-hardening artifact in the posterior fossa and inability to perform scans in multiple planes (16–18).

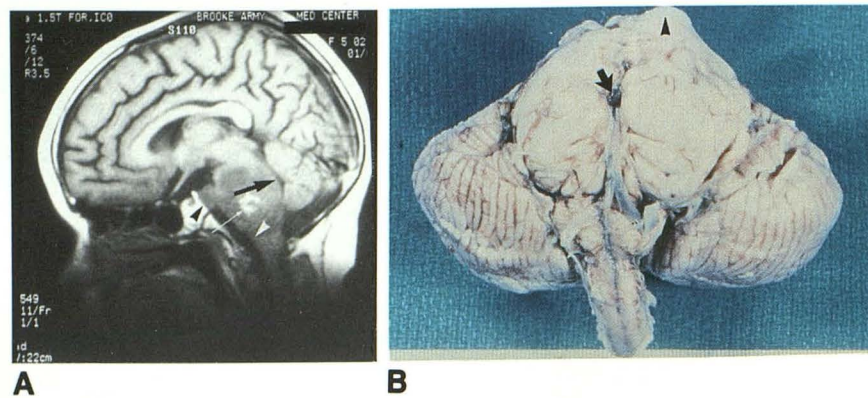


Fig. 4. A, Sagittal T1-weighted nonenhanced image 1 day before death (SE 600/27) illustrates hypointense pons. The enlarged pons obliterates the normal pontomedullary angle (*white arrowhead*) and the pontine tegmentum has become convex posteriorly (*large arrow*). The central pontine focus of high signal again suggests hemorrhage (*small white arrow*). A focal exophytic component of tumor extends into prepontine cistern just posterior to the clivus (*black arrowhead*).

B, Gross specimen confirms symmetrical nodular enlargement of the pons which encases the basilar artery (*arrow*) as seen in Figs 3B and 3C. The focal exophytic component (*black arrowhead*) is again seen.

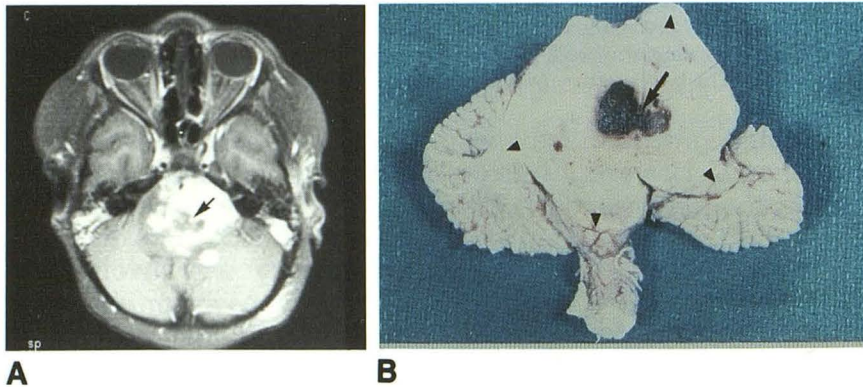


Fig. 5. A, Axial T1-weighted (SE 600/27) gadolinium-enhanced image through the pons from the same MR scan as Figs 3 and 4 demonstrates marked enhancement in the pons with a central, dumbbell-shaped, nonenhancing region consistent with hemorrhage and necrosis (*black arrow*) as seen in B.

B, Section through the pons confirms dumbbell-shaped acute central pontine hematoma (*black arrow*) evident on MR images, as well as extension of the whiteish to pale gray tumor into the medulla, midbrain, and middle cerebellar peduncles (*arrowheads*).

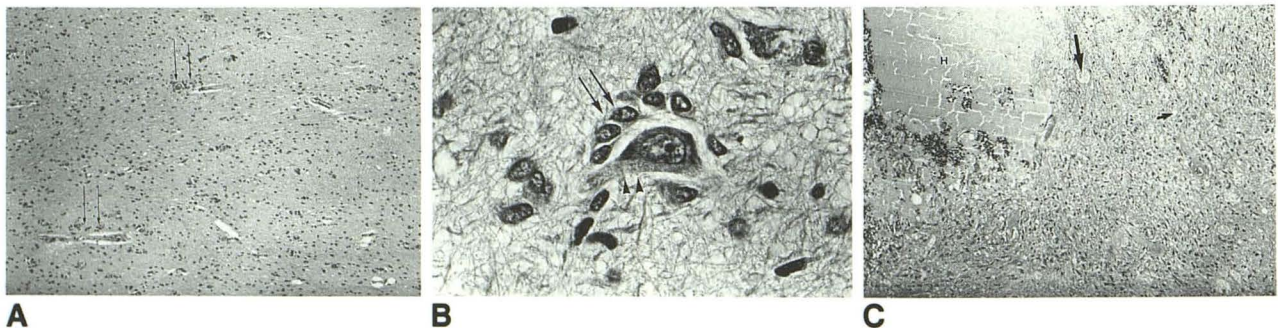


Fig. 6. A, Low-power (100X, hematoxylin and eosin stain) photomicrograph demonstrates widely dispersed small astrocytic tumor cells tracking along nerve axons and vessels (*arrows*).

B, High-power (400X) view demonstrating small tumor cells containing enlarged, irregular hyperchromatic nuclei (*long black arrows*) surrounding a neuron (malignant satellitosis) and its axon (*arrowheads*).

C, Low-power (100X) view of area of necrosis and hemorrhage. There is dissolution of the walls of small vessels (*arrowhead*) and a loss of normal glial parenchymal cells (neuropil), as well as the presence of ghost cells (*small black arrow*) and an extensive area of parenchymal hemorrhage (*H*) in the upper left portion of the photomicrograph.

The delayed effects of radiation and chemotherapy include injury to the endothelial lining of small blood vessels, eventually resulting in ischemia, infarction, necrosis, and damage to the blood-brain barrier. These effects can occur months after radiation therapy. The late onset of enhancement after gadolinium administration, therefore, is common and often coincides with the recurrence of symptoms (15).

Functional Brain Imaging

The onset of enhancement after treatment of an initially nonenhancing brain stem glioma can pose a diagnostic dilemma. ^{201}Tl -SPECT can be useful in distinguishing between recurrent tumor and nonneoplastic lesions such as radiation necrosis, resolving hematoma, or postsurgical change. Normal brain and nonneoplastic lesions within the central nervous system show little or no ^{201}Tl uptake. ^{201}Tl -SPECT imaging can thus be used in lieu of biopsy to establish tumor regrowth or to guide biopsy or additional treatment by localizing areas of greatest radionuclide uptake (19, 20).

Differential Diagnosis

The differential diagnosis of brain stem astrocytoma includes encephalitis, tuberculoma, vascular malformation, and resolving hematoma. Because of the characteristic signal of blood and blood breakdown products, MR can differentiate brain stem glioma from vascular malformations and hemorrhage. A lack of mass effect on MR scan combined with an appropriate clinical history may be more suggestive of an infectious rather than a neoplastic lesion etiology (21, 22). Stereotactic techniques have reduced the morbidity and mortality of biopsy and improved the accuracy of biopsy in achieving an initial histologic diagnosis. Biopsy may be indicated in cases in which the distinction between brain stem neoplasm and infection is clinically unclear (23, 24).

Summary

This case demonstrated the classic gross, pathologic, CT, and MR findings of pontine astrocytoma. The role of functional brain im-

aging in identifying regrowth of tumor was illustrated and the differential diagnosis of a brain stem lesion summarized.

References

1. Segall HD, Zee CS, Naidich TP, et al. Computed tomography in neoplasms of the posterior fossa in children. *Radiol Clin North Am* 1982;20:237-253
2. Farwell JR, Dohrmann GJ, Flannery JT. Central nervous system tumors in children. *Cancer* 1977;40:3123-3132
3. Lassman LP, Arjona VE. Pontine gliomas of childhood. *Lancet* 1967;1:913-915
4. Panitch HS, Berg BO. Brain stem tumors of childhood and adolescence. *Am J Dis Child* 1970;119:465-472
5. Fulton DS, Levin VA, Wara WM, et al. Chemotherapy of pediatric brain-stem tumors. *J Neurosurg* 1981;54:721-725
6. Flores LE, Williams DL, Bell BA, O'Brien M, Ragab AH. Delay in diagnosis of pediatric brain tumors. *Am J Dis Child* 1986;140:684-686
7. Martin RA, Handel SF, Aldama AE. Inability to sneeze as a manifestation of medullary neoplasm. *Neurology* 1991;41:1675-1676
8. Naidich TP, Zimmerman RA. Primary brain tumors in children. *Semin Roentgenol* 1984;19:100-114
9. Buckley RC. Pontine gliomas: a pathologic study and classification of twenty-five cases. *Arch Pathol* 1930;9:779-819
10. Pilcher C. Spongioblastoma polare of the pons. *Arch Neurol Psychiatr* 1934;1210-1230
11. Lassiter KRL, Alexander E Jr, David CH Jr, et al. Surgical treatment of brainstem gliomas. *J Neurosurg* 1971;34:719-725
12. Stroink AR, Hoffman HJ, Hendrick EB, Humphreys RP, Davidson G. Transpendymal benign dorsally exophytic brain stem gliomas in childhood: diagnosis and treatment recommendations. *Neurosurgery* 1987;20:439-444
13. Albright AL, Guthkelch AN, Packer RJ, Price RA, Rourke LB. Prognostic factors in pediatric brainstem gliomas. *J Neurosurg* 1986;65:751-755
14. Stroink AR, Hoffman HJ, Hendrick EB, Humphreys RP. Diagnosis and management of pediatric brain stem gliomas. *J Neurosurg* 1986;65:745-750
15. Ball WS Jr, Prenger EC, Ballard ET. Neurotoxicity of radio/chemotherapy in children: pathologic and MR correlation. *AJNR: Am J Neuroradiol* 1992;13:761-776
16. Byrne JV, Kendall BE, Kingsley DP, Moseley IF. Lesions of the brain stem: assessment by magnetic resonance imaging. *Neuroradiology* 1989;31:129-133
17. Lee BCP, Kneeland JB, Walker RW, et al. MR imaging of brainstem tumors. *AJNR: Am J Neuroradiol* 1985;6:159-163
18. Hueftle MG, Hans JS, Kaufman B, et al. MR imaging of brainstem gliomas. *J Comput Assist Tomogr* 1985;9:263-267
19. Kaplan WD, Takvorian T, Morris JH, et al. Thallium-201 brain tumor imaging: a comparative study with pathologic correlation. *J Nucl Med* 1987;28:47-52
20. Mountz JM, Stafford-Schuck K, McKeever PE, et al. Thallium-201 tumor/cardiac ratio estimation of residual astrocytoma. *J Neurosurg* 1988;68:705-709
21. Bradley WG Jr. Hemorrhage and brain iron. In: Stark DD, Bradley WG Jr, eds. *Magnetic resonance imaging*. 2nd ed. St. Louis: Mosby, 1992:721-769
22. Barhovich AJ. *Pediatric neuroimaging*. New York: Raven, 1990:164
23. Abernathy CD, Camacho A, Kelly PJ. Stereotaxic suboccipital transcerebellar biopsy of pontine mass lesions. *J Neurosurg* 1989;70:195-200
24. Reigel DH, Scarff TB, Woodford JE. Biopsy of pediatric brain stem tumors. *Childs Brain* 1979;5:329-340